

**“Highly efficient and unidirectional energy transfer within a tightly self-assembled host–guest multichromophoric array”**

Nikolaos Karakostas, Irene M. Mavridis, Kostas Seintis, Mihalis Fakis,  
Eftychia N. Koini ,Ioannis D. Petsalakis and George Pistolis\*

<b>Table of Contents</b>	<b>page</b>
<b>Materials and Methods</b>	<b>S2</b>
<b>Synthesis of Bodipy 1; <sup>1</sup>H NMR, <sup>13</sup>C NMR</b>	<b>S3</b>
<b>Self-assembly of Rhomboid (12)<sub>2</sub>, <sup>1</sup>H NMR of (12)<sub>2</sub></b>	<b>S4</b>
<b><sup>31</sup>P{<sup>1</sup>H} NMR of (12)<sub>2</sub></b>	<b>S5</b>
<b><sup>1</sup>H-<sup>1</sup>H COSY of (12)<sub>2</sub></b>	<b>S6</b>
<b><sup>1</sup>H-<sup>1</sup>H ROESY of (12)<sub>2</sub></b>	<b>S7</b>
<b><sup>1</sup>H DOSY of (12)<sub>2</sub></b>	<b>S8</b>
<b>Molecular model of (12)<sub>2</sub></b>	<b>S9</b>
<b>ESI-MS of (12)<sub>2</sub></b>	<b>S10</b>
<b>Inclusion complex 4Spy ⊂ (12)<sub>2</sub></b>	<b>S12</b>
<b><sup>1</sup>H NMR of 4Spy ⊂ (12)<sub>2</sub></b>	<b>S13</b>
<b><sup>1</sup>H-<sup>1</sup>H NOESY of 4Spy ⊂ (12)<sub>2</sub></b>	<b>S14</b>
<b>Spectroscopic data of the compounds 1, 2, (12)<sub>2</sub>, 4SPy and 4SPy ⊂ (12)<sub>2</sub></b>	<b>S15</b>
<b>Femtosecond Upconversion</b>	<b>S17</b>
<b>Theoretical Calculations</b>	<b>S18</b>
<b>Chromophoric arrangement and dipole moments orientation</b>	<b>S20</b>
<b>X-ray Crystal Structure Determination</b>	<b>S21</b>
<b>References:</b>	<b>S22</b>

**Materials and Methods:** All chemicals were used without further purification and purchased from commercial sources as follows: 4-ethynylpyridine hydrochloride (Aldrich), tert-butyllithium 1.7 M in pentane (Aldrich). Compound **2** was prepared according to literature procedures.<sup>1</sup> 1,3,6,8-Pyrenetetrasulfonic acid tetrasodium salt (Aldrich) was converted to the tetrabutylammonium salt **4SPy** with tetrabutylammonium hydroxide in CH<sub>2</sub>Cl<sub>2</sub>, then washed with water until neutral pH. THF was distilled over Na / benzophenone, CHCl<sub>3</sub> and CDCl<sub>3</sub> were distilled over CaH<sub>2</sub>, DMF was distilled under reduced pressure.

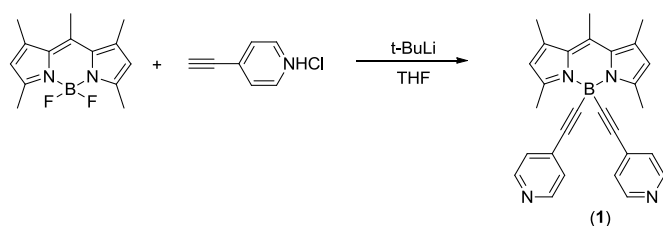
NMR spectra were recorded on a Bruker Avance DRX 500 spectrometer. <sup>1</sup>H and <sup>13</sup>C chemical shifts are reported relative to residual solvent signals, and <sup>31</sup>P{<sup>1</sup>H} chemical shifts are referenced to an external 85% H<sub>3</sub>PO<sub>4</sub> (δ 0.00 ppm) sample. DOSY NMR experiments were carried out with solutions of 4 cm height to ensure gradient linearity along the samples. The temperature was controlled with a 135 L/min air flow and kept at 298.0 ± 0.1 K. Data were acquired with 32 scans for each gradient step, 4 dummy scans and a linear gradient of 32 steps between 2% and 95%. Processing was carried out with Bruker's Topspin 2.1 software.

Absorption spectra were recorded on a Perkin-Elmer Lambda-16 spectrophotometer. Steady-state fluorescence spectra were performed by Perkin-Elmer model LS-50B and Edinburgh Instruments model FS-900 spectrophotometers. Fluorescence lifetimes (τ) were determined using the time correlated single-photon counter FL900, of the Edinburgh Instruments spectrophotometer. Fluorescence quantum yield measurements of the Bodipy-based compounds in chloroform (η(CHCl<sub>3</sub>) = 1.445) were obtained relative to Rhodamine 6G in ethanol (Φ=0.94, η(EtOH) = 1.358).<sup>2</sup> The quantum yield of the pyrene's derivative was measured relative to an aqueous solution of quinine sulphate containing 1N H<sub>2</sub>SO<sub>4</sub> (Φ = 0.546)<sup>3</sup>

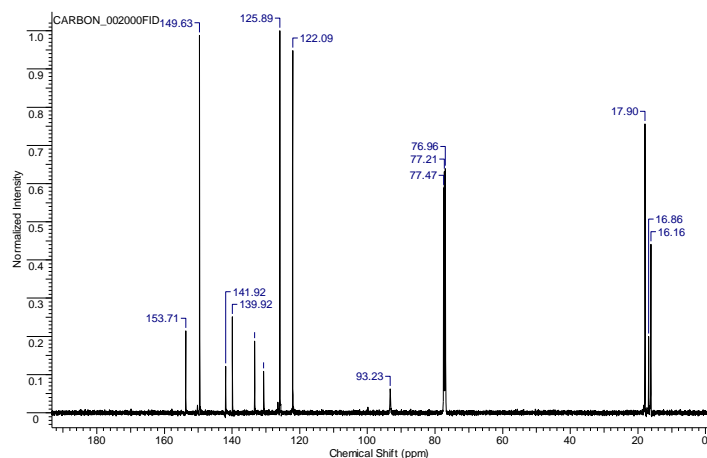
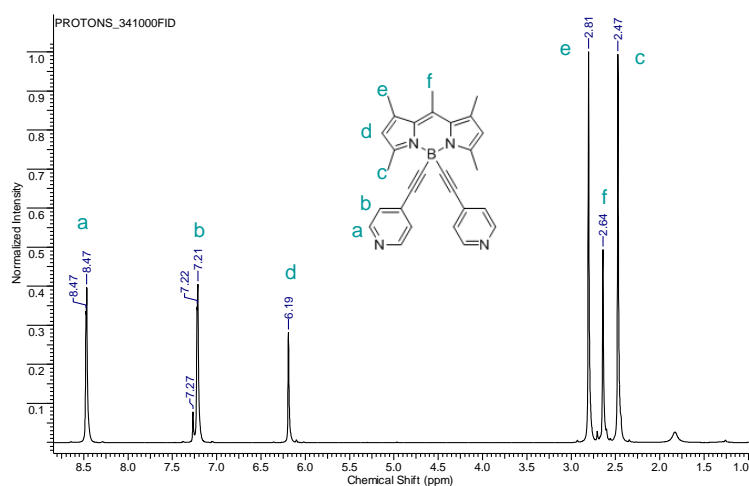
The fluorescence dynamics in the fs to ps timescale were obtained using a femtosecond time resolved upconversion system described in details elsewhere.<sup>4,5</sup> The fundamental beam of a mode-locked Ti:Sapphire laser at 760nm with 80fs pulse duration has been frequency doubled through a BBO crystal. The second harmonic, at 380nm, was used for the excitation of the samples while the fundamental beam was used as the gate beam. The excitation power was typically below 5mW. For avoiding thermal degradation, the samples were placed in a rotating holder. The fluorescence of the samples and the gate beam were focused on a second BBO crystal to generate an upconversion beam (type I phase matching). This beam passed through appropriate filters and a monochromator and it was detected through a photomultiplier. The temporal resolution of the technique was ~140fs and the decays were taken under magic angle conditions.

Electrospray ionization mass spectrometry (ESI-MS) was performed on a LTQ Orbitrap Velos (Thermo Fisher, San Jose, USA) equipped with a heated ESI probe, in the positive ionization mode. Samples were dissolved in acetone/dichloromethane 1/1 and 100 µg/ml solutions were infused at a flow rate of 5 µl/min. The resolution of the Orbitrap mass analyzer was set to 100000 and 100 scans were averaged.

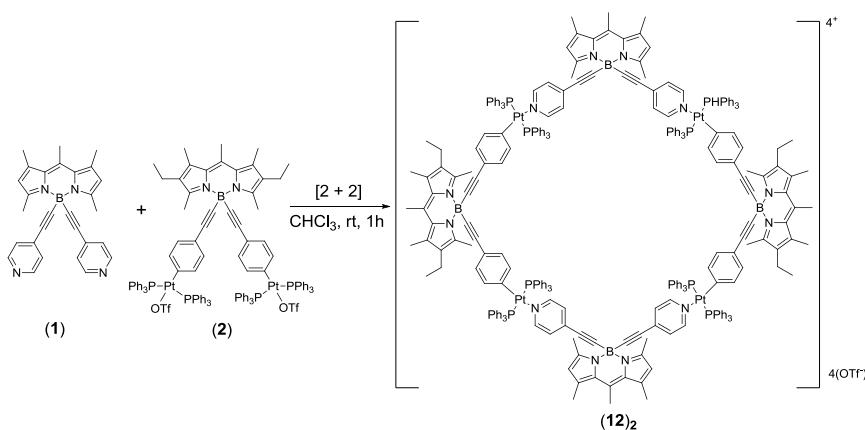
## Synthesis of Bodipy 1.



In a Schlenk flask, tert-butyllithium (1 ml, 1.7 mmol) was added dropwise at  $-78\text{ }^{\circ}\text{C}$  to a stirred solution of 4-ethynylpyridine hydrochloride (117.5 mg, 0.842 mmol) in 30 ml of anhydrous THF under Ar. The mixture was stirred at  $-78\text{ }^{\circ}\text{C}$  for 20 min and at room temperature for another 1.5 h. The precursor Bodipy6 (88.3 mg, 0.337 mmol) was dissolved in 15 ml of anhydrous THF under Ar and added to the lithium acetylide mixture through a pressure equalising dropping funnel. After 10 min the reaction was stopped with water, extracted with  $\text{CH}_2\text{Cl}_2$  and washed 3 times with water. The organic layer was dried with  $\text{Na}_2\text{SO}_4$  and after evaporation of the solvents purified by silica gel column chromatography with eluent EtOAc. Recrystallization from EtOAc gave 40 mg (0.093 mmol) of bright orange crystals (Yield 28%).  $^1\text{H}$  NMR ( $\text{CDCl}_3$ ):  $\delta$  8.47 (d,  $J=4.1$  Hz, 4H, Ha-Py),  $\delta$  7.22 (d,  $J=4.1$  Hz, 4H, Hb-Py), 2.81 (s, 6H), 2.64 (s, 3H), 2.47 (s, 6H);  $^{13}\text{C}$  NMR ( $\text{CDCl}_3$ ): 153.71, 149.63, 141.92, 139.92, 133.37, 130.66, 125.89, 122.09, 93.23, 17.90, 16.86, 16.16; Anal. Calcd for  $\text{C}_{28}\text{H}_{25}\text{BN}_4$ : C, 78.51; H, 5.88; N, 13.08. Found: C, 77.85; H, 5.84; N, 13.01;



### Self-assembly of Rhomboid (12)<sub>2</sub>.



5.1 mg (0.012 mmol) of 1 were dissolved in 2.5 ml of CHCl<sub>3</sub> in a 20 ml vial. A solution of 27.2 mg (0.012 mmol) of 2 in 2.5 ml CHCl<sub>3</sub> was added to the vial in 10 min with continuous stirring at rt for one more hour. Microcrystalline solid, free of higher order oligomers, was obtained when the volume of the solution was reduced to 1 ml with a stream of Ar, and 1 ml of DMF was added followed by slow diffusion of EtOAc. The solid was washed twice with Et<sub>2</sub>O and dried for 8 hours with an oil pump. Yield 79.0% (25.1 mg or 0.0047 mmol). <sup>1</sup>H NMR (CDCl<sub>3</sub>): δ 7.97 (d, J=5.0 Hz, 8H), 7.30 (s), 6.62 (d 5.0 Hz, 8H), 6.54 (d, 7.4 Hz, 8H), 6.36 (d 7.4 Hz, 8H), 6.20 (s, 4H), 2.72 (s, 12H), 2.62 (s), 2.60 (s), 2.57 (s), 2.46(m, 20H), 2.34 (s, 12H), 1.07 (t, J=6.9 Hz, 12H); Anal. Calcd for C<sub>272</sub>H<sub>236</sub>B<sub>4</sub>F<sub>12</sub>N<sub>12</sub>O<sub>12</sub>P<sub>8</sub>Pt<sub>4</sub>S<sub>4</sub>: C, 61.73; H, 4.49; N, 3.18. Found: C 61.8, H 4.9, N 3.5.

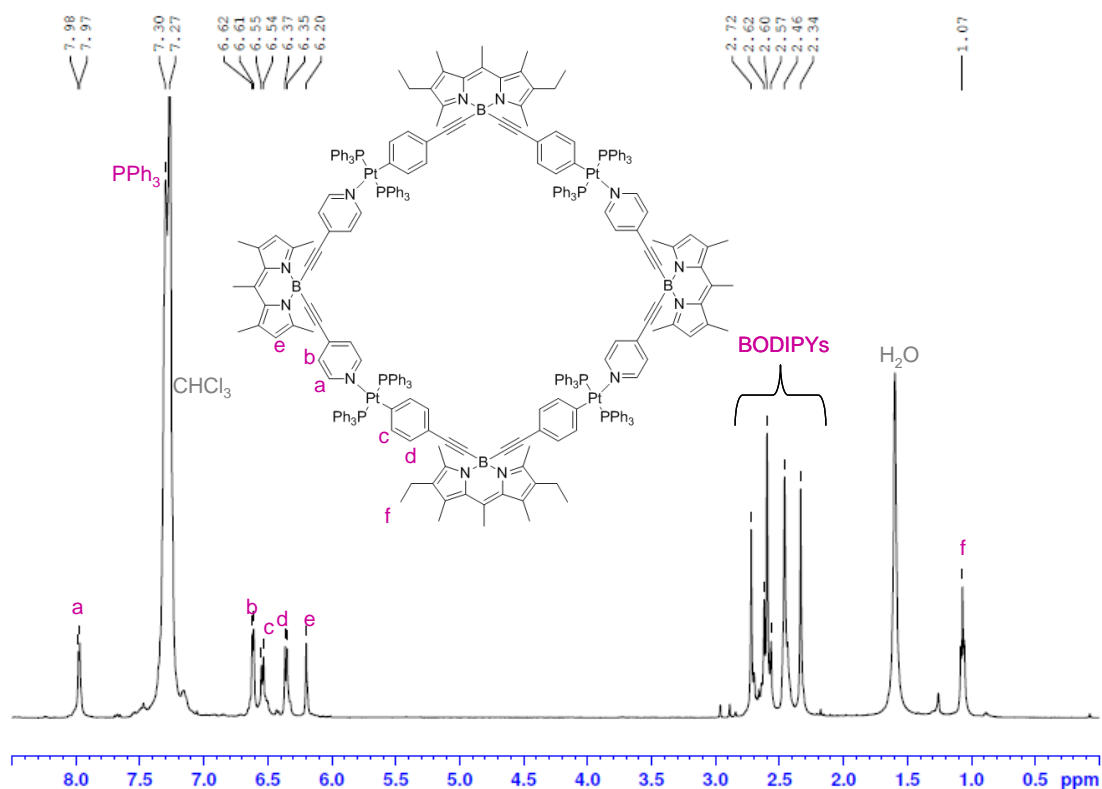
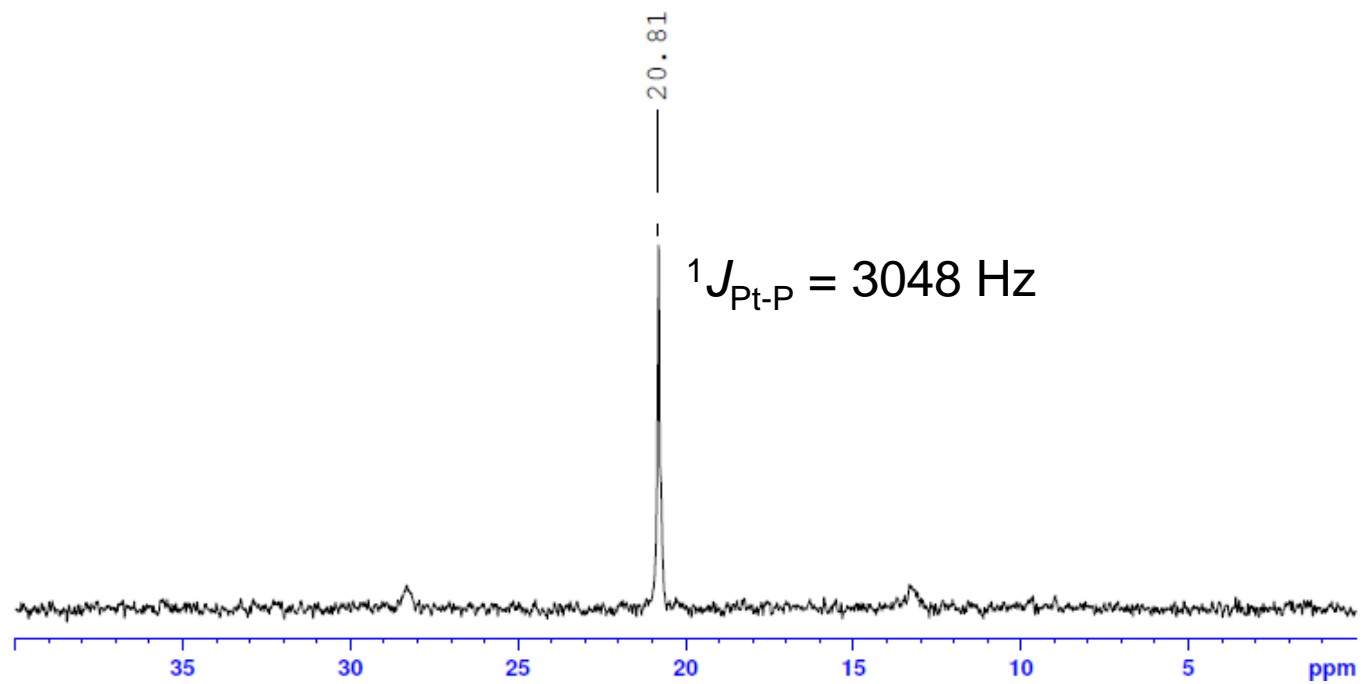
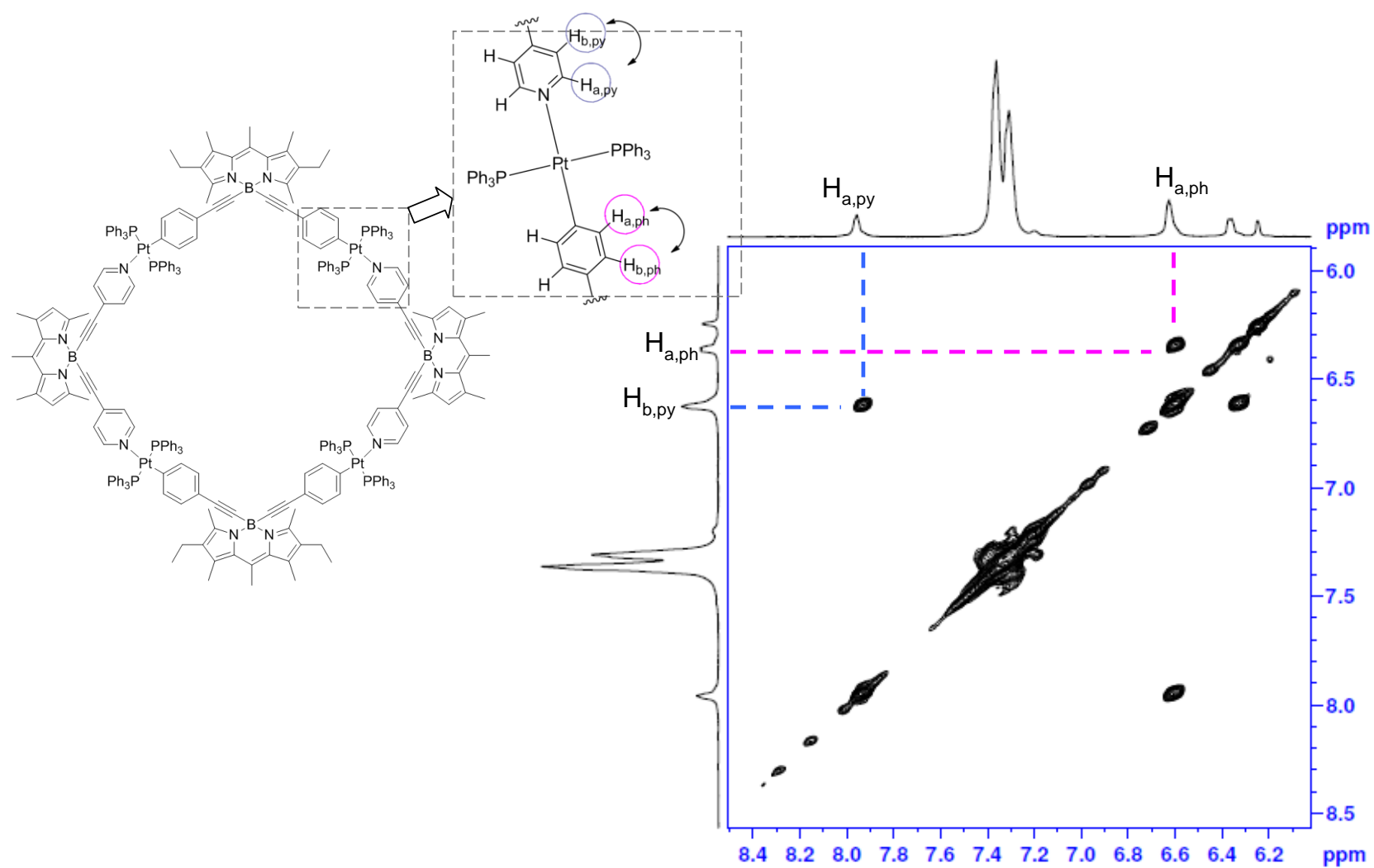


Figure S3. <sup>1</sup>H NMR (500 MHz) spectrum of (12)<sub>2</sub> in CDCl<sub>3</sub>.



**Figure S4.**  $^{31}\text{P}$  { $^1\text{H}$ } NMR (121.4 MHz) spectrum of **(12)**<sub>2</sub> in  $\text{CD}_2\text{Cl}_2$ .



**Figure S5.**  $^1\text{H}$ - $^1\text{H}$  COSY (500 MHz, 298 K,  $\text{CD}_2\text{Cl}_2$ ) spectrum of  $(12)_2$ .

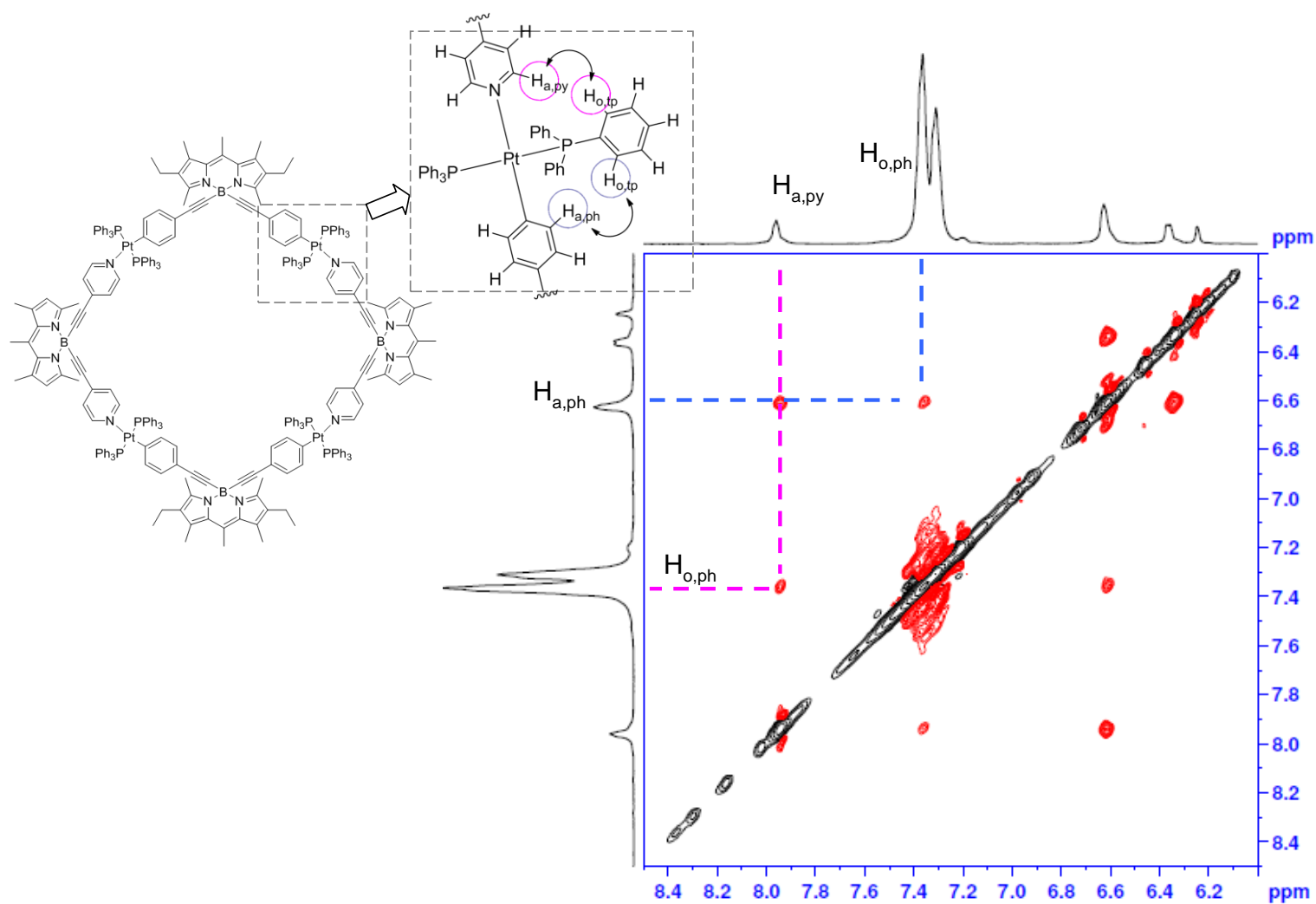


**Figure S6.**  $^1\text{H}$ - $^1\text{H}$  ROESY (500 MHz, 298 K,  $\text{CD}_2\text{Cl}_2$ ) spectrum of  $(12)_2$ .

### $^1\text{H}$ DOSY - SPECTRA

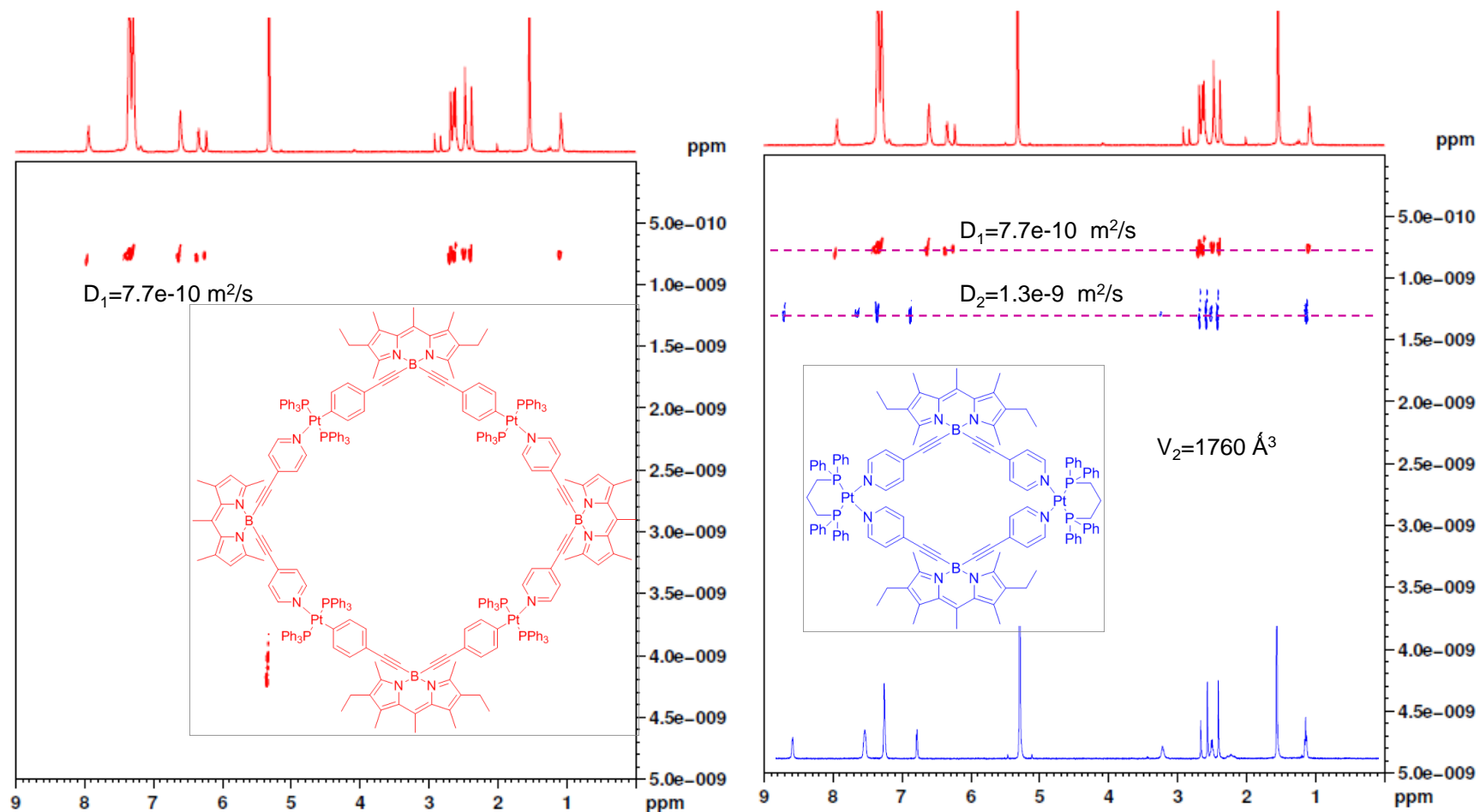


**Figure S7.** To correct as much as possible for shape effects we compared the  $^1\text{H}$  DOSY spectrum (500 MHz,  $\text{CD}_2\text{Cl}_2$ , 298 K) of the present assembly  $(\mathbf{12})_2$  (red) with the one of a similar rhomboidal cavitanid<sup>1</sup> for which the explicit structure has been obtained by x-ray crystallography (right, blue) ( $V_2 = 1760 \text{ \AA}^3$ ). For a spherical molecule the diffusion coefficient  $D$  is described by the Stokes-Einstein equation:

$$D = \frac{kT}{6\pi\eta r_s}$$

where  $k$  is the Boltzmann constant,  $T$  the temperature,  $\eta$  the viscosity of the solvent and  $r_s$  the hydrodynamic radius of the molecule. For a set of two molecules at the same temperature and solvent we have:

$$\frac{r_{s1}}{r_{s2}} = \frac{D_2}{D_1} \Rightarrow r_{s1} = r_{s2} \frac{D_2}{D_1}$$

The volume  $V$  of a sphere is  $V=4\pi r^3 / 3$ , therefore:

$$r_{s1} = \frac{D_2}{D_1} \sqrt[3]{\frac{3}{4\pi} V_2} \Rightarrow r_{s1} = 12.7 \text{ \AA}$$

This value is comparable to the size determined by molecular modeling.

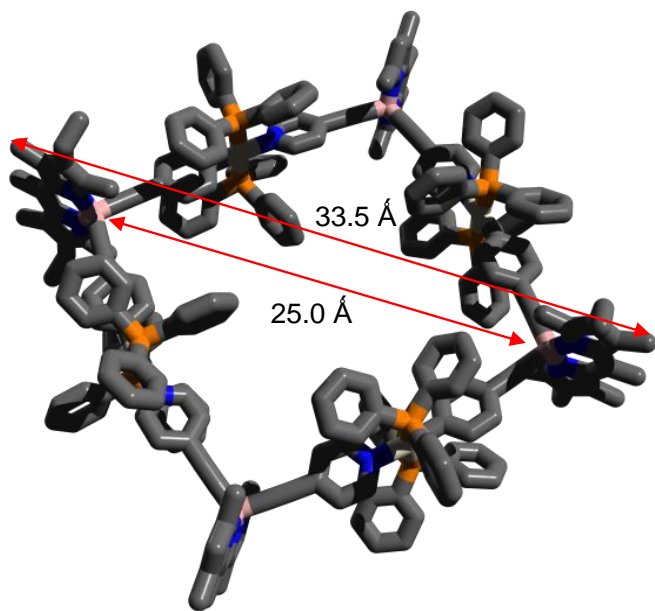


**Figure S8.** Molecular model of  $(12)_2$  using the MOPAC2012 program<sup>7</sup> and PM6 semiempirical method with the MOZYME function.

### High-resolution electrospray ionization mass spectrometry (ESI-MS)

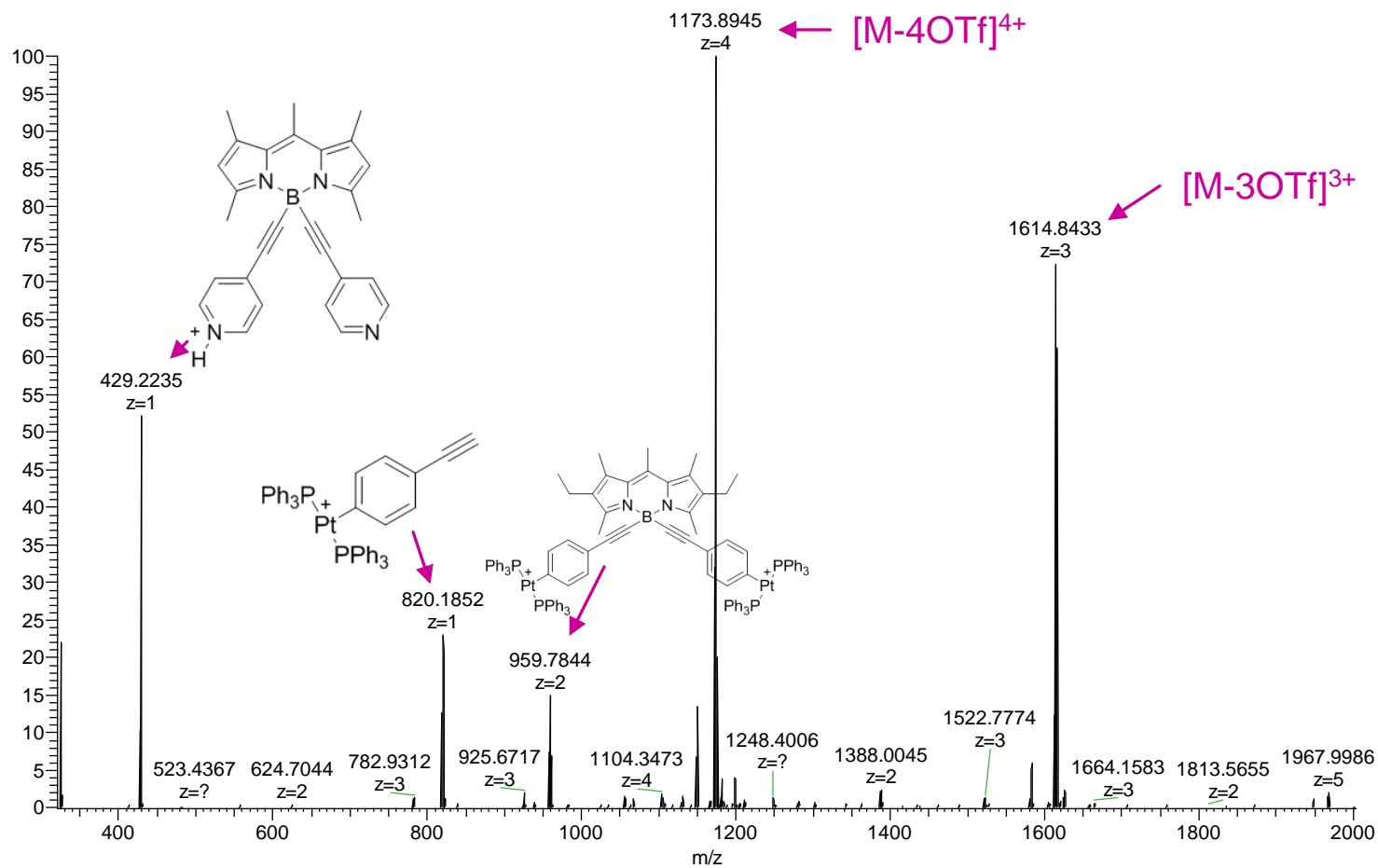
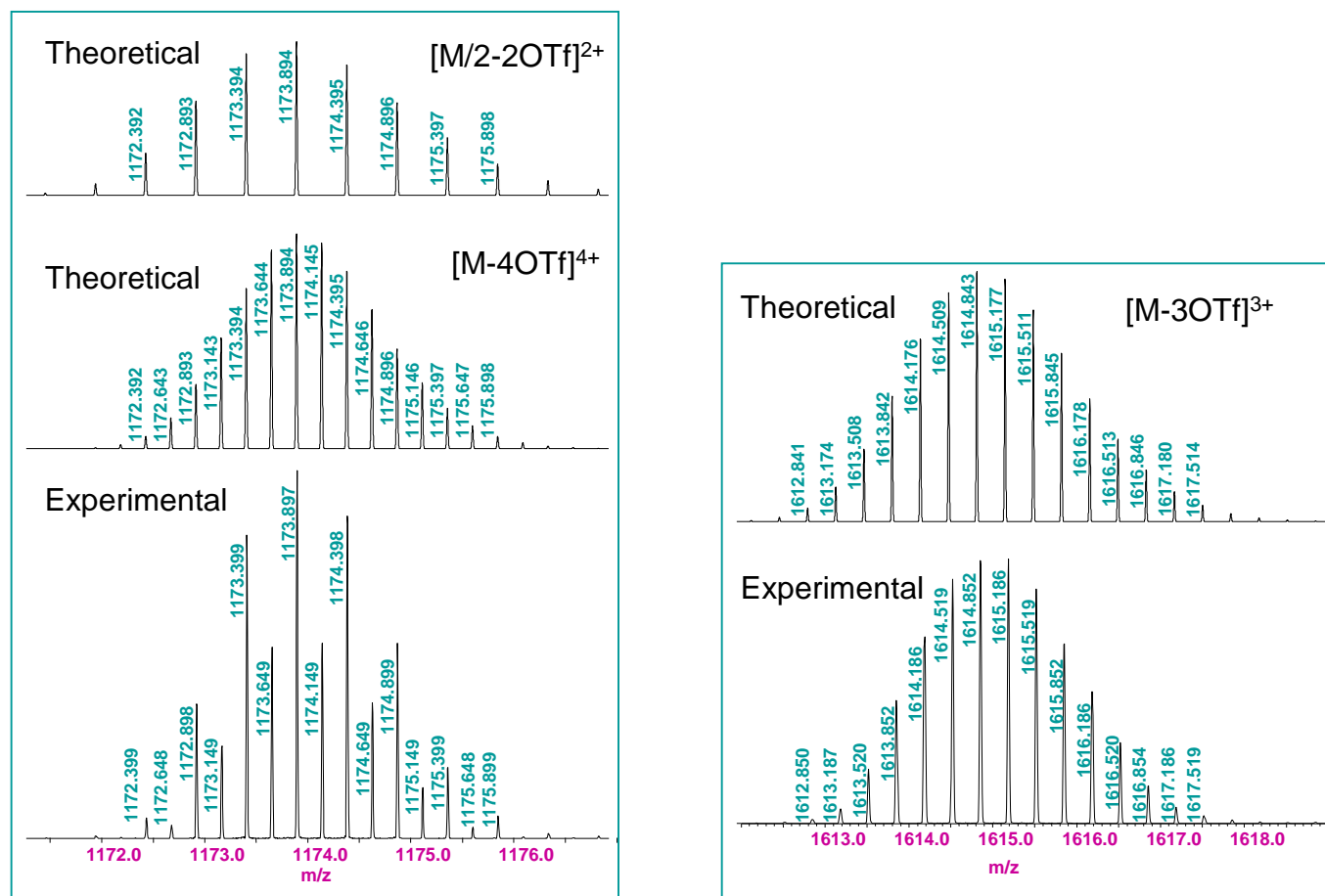
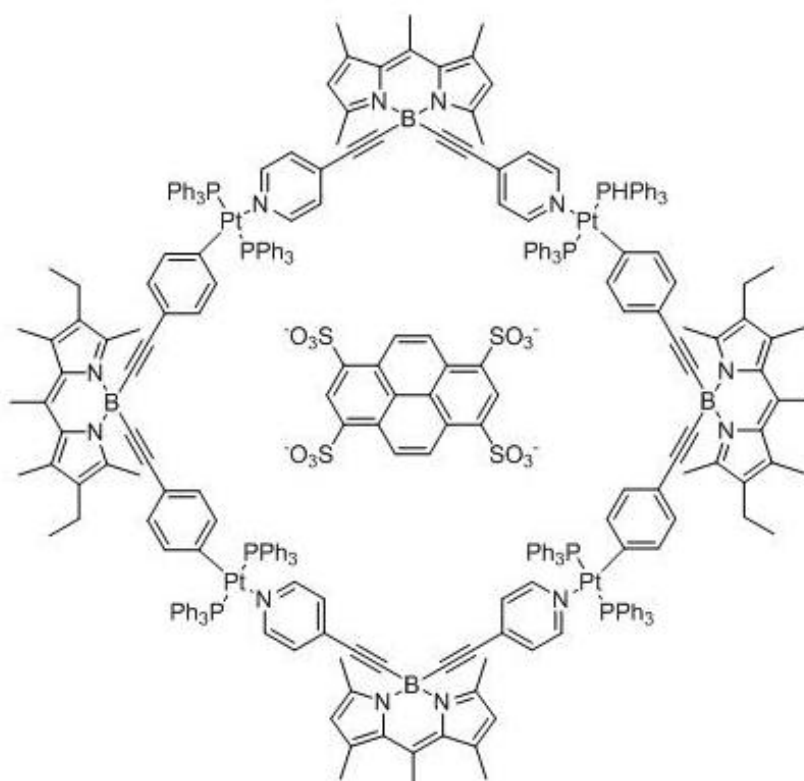


Figure S9. ESI-MS of (12)<sub>2</sub>.



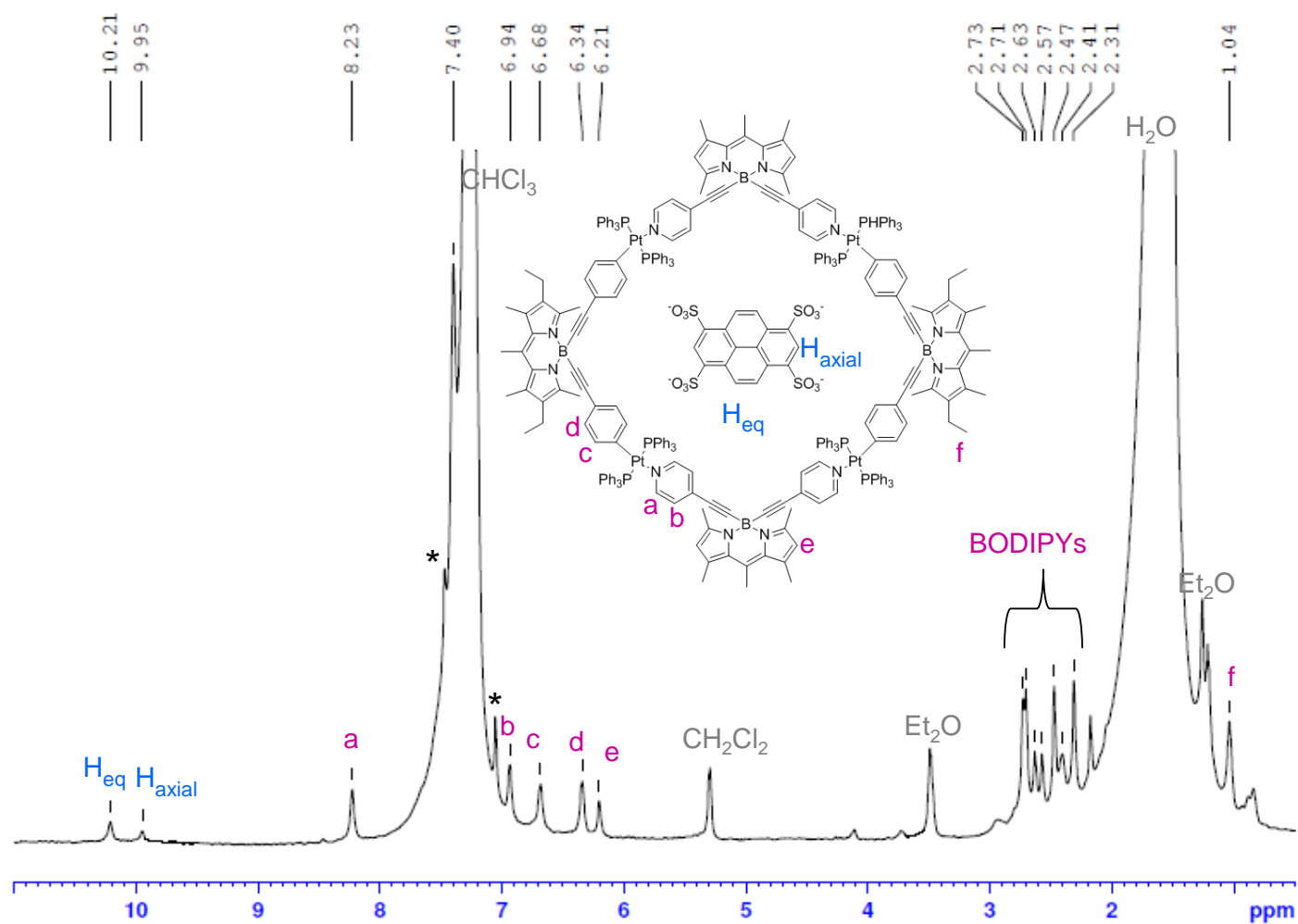
**Figure S10.** ESI-MS of (12)<sub>2</sub>. The isotopic distribution shows that the quadruply charged molecular ion of (12)<sub>2</sub> is superimposed with the doubly charged fragmentation product of the structure having half the mass. The fragment is generated during the ESI process. The symmetry of [M-3OTf]<sup>3+</sup> excludes such an overlap.

### Inclusion complex $4\text{SPy} \subset (\mathbf{12})_2$



2.6 mg ( $4.9 \times 10^{-4}$  mmol) of  $(\mathbf{12})_2$  were dissolved with 1 ml of DMF/ $\text{CHCl}_3$  1/1 solution in a 5 ml vial. 195  $\mu\text{l}$  of a  $2.5 \times 10^{-3}$  M solution of  $4\text{SPy}$  in  $\text{CHCl}_3$  ( $4.9 \times 10^{-4}$  mmol) were added to the vial. X-ray quality crystals were grown when EtOAc was allowed to diffuse.

For NMR characterization the mother liquid was drained and the solid was dried with an oil pump for 6 h. The orange material was washed twice with 2 ml  $\text{CH}_2\text{Cl}_2/\text{Et}_2\text{O}$  1/1 and dried with an Ar stream.  $^1\text{H}$  NMR ( $\text{CDCl}_3$ ):  $\delta$  10.21, 9.95, 8.23, 7.40, 6.94, 6.69, 6.34, 6.21, 2.73, 2.71, 2.63, 2.58, 2.48, 2.41, 2.31, 1.04



\* CHCl<sub>3</sub> satellite peak

**Figure S11.** Full <sup>1</sup>H NMR (500 MHz) spectrum of (12)<sub>2</sub>c4SPy (~4 × 10<sup>-5</sup> M) in CDCl<sub>3</sub>.

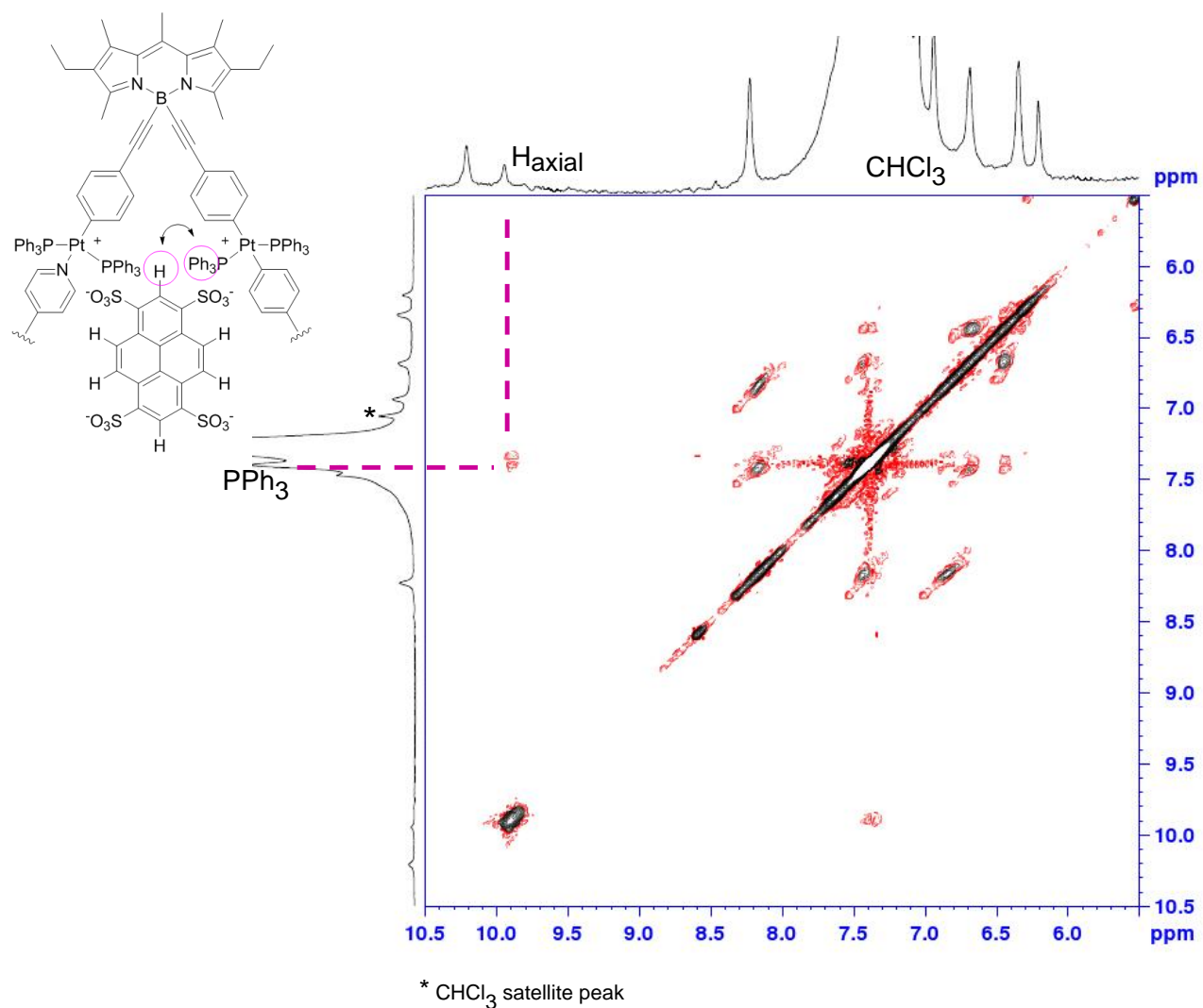


**Figure S12.**  $^1H$ - $^1H$  NOESY (500 MHz, 298 K, CDCl<sub>3</sub>) spectrum of  $(12)_2c4SPy$ .

**Additional Spectroscopic data of the compounds **1**, **2**, (**12**)<sub>2</sub>, **4SPy** and **4SPy** ⊂ (**12**)<sub>2</sub>**

**Table S1.** Spectroscopic data of **1**, **2**, (**12**)<sub>2</sub> and **4SPy** ⊂ (**12**)<sub>2</sub> in CHCl<sub>3</sub> at 23<sup>0</sup> C.

	$\lambda_{abs}^{max}$ (nm) <sup>a</sup> ( $\epsilon$ M <sup>-1</sup> cm <sup>-1</sup> )	$\lambda_{fl}$ (nm) <sup>b</sup>	$\Phi_f$ <sup>c</sup>	$\tau$ (ns) <sup>d</sup>
<b>1</b>	497 (90800)	510	0.92	5.56
<b>2</b>	516 (77300)	534	0.86	6.40
( <b>12</b> ) <sub>2</sub>	497 (93250)	536	0.86	6.40
<b>4SPy</b>	379 (62400)	385	0.24	5.06
<b>4SPy</b> ⊂( <b>12</b> ) <sub>2</sub>	497 (93250)	538	0.74 (ex: 380 nm) 0.84 (ex: 465 nm)	6.35

(a)  $\lambda_{max}$  of the absorption spectrum and extinction coefficient ( $\epsilon$ ) at  $\lambda_{max}$ . (b) Maximum wavelength of fluorescence (c) Fluorescence quantum yield. (d) Fluorescence lifetime.

- The *transition dipole moment* ( $\mu$ ) for a given transition was calculated from the spectra using the relation of the dipole strength<sup>8</sup> (D);

$$D = \left| \vec{\mu} \right|^2 = 9.186 \times 10^{-3} n f^{-2} \int \frac{\epsilon(\tilde{\nu})}{\tilde{\nu}} d\tilde{\nu}$$

where  $n$  is the refractive index and  $f$  is the local-field correction factor.

S<sub>0</sub>→S<sub>1</sub>: For Bodipys **1** and **2**  $\mu_1^{S1} = \mu_2^{S1} = 6.4$  D; for **4SPy**;  $\mu_p^{S1} = 3.7$  D.

S<sub>0</sub>→S<sub>2</sub>:  $\mu_1^{S2} = 3.2$  D,  $\mu_2^{S2} = 3.1$  D

- The *overlap integral* ( $J_{AB}^{state}$ ) for a pair of chromophores A and B, was calculated from the absorption and the emission spectra.<sup>9</sup>

$$J_{12}^{S1} = 0.0136 \text{ cm};$$

$$J_{P1}^{S1} = 4.7 \times 10^{-4} \text{ cm}; \quad J_{P2}^{S1} = 2.5 \times 10^{-4} \text{ cm}$$

$$J_{P2}^{S2} = 7.1 \times 10^{-3} \text{ cm}; \quad J_{P1}^{S2} = 2.5 \times 10^{-3} \text{ cm}$$

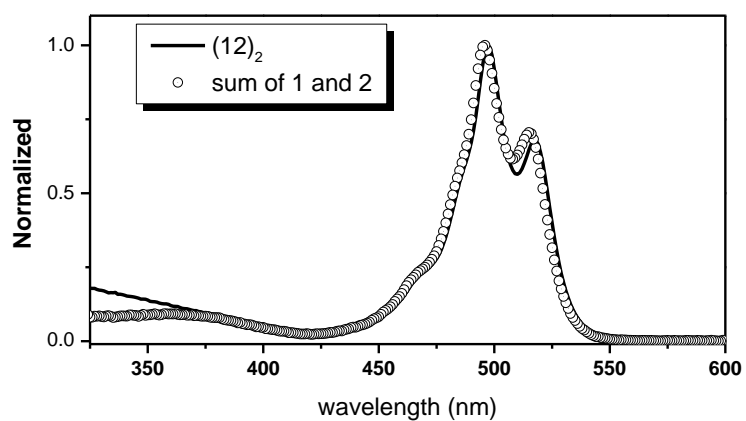


**Figure S13a.** Normalized absorption spectra of the cavitand  $(12)_2$  and of the sum (x 2) of the absorption spectra of the individual components **1** and **2**.

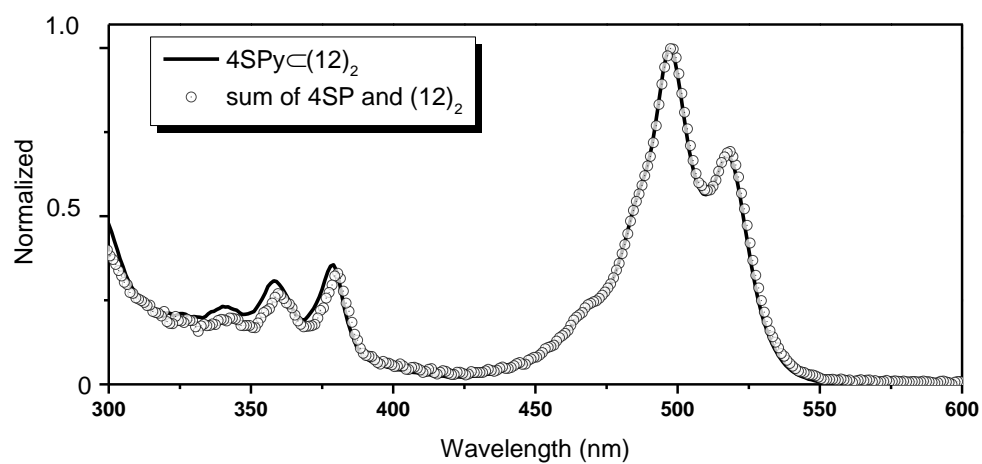


**Figure S13b.** Normalized absorption spectra of the inclusion complex  $4SPy\subset(12)_2$  and of the sum of the absorption spectra of **1** (x 2), **2** (x 2) and **4SPy**.

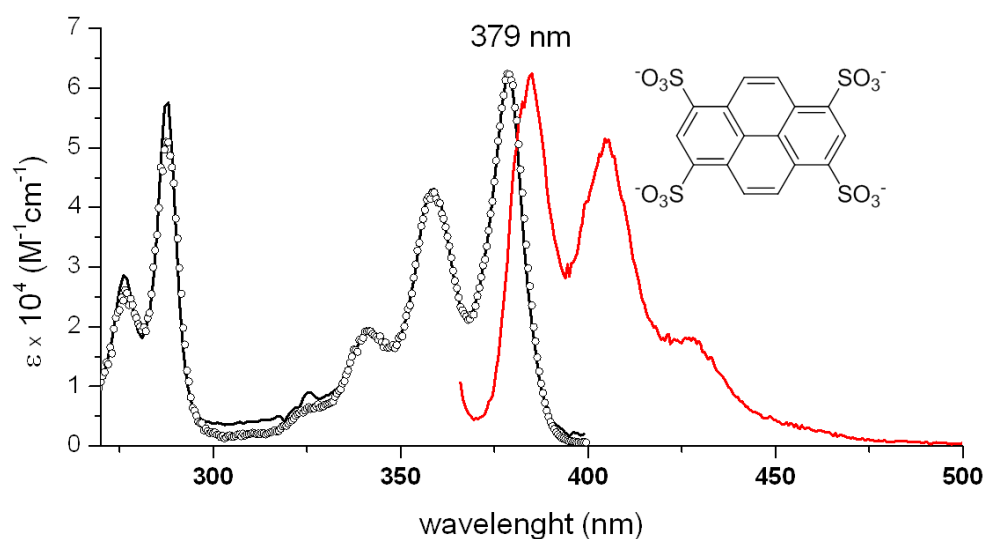


**Figure S14a.** Absorption (solid-line), fluorescence excitation (open circles; em: at 420 nm) and fluorescence spectra (exc: at 360 nm) of **4SPy** in  $\text{CHCl}_3$ .

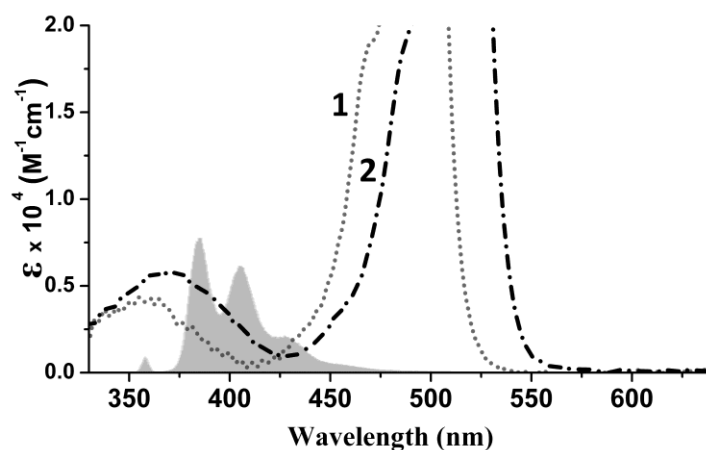


**Figure S14b.** Spectral overlap between the emission spectrum of **4SPy** and the absorption spectra of Bodipy **1** and **2** of the host: good spectral overlap is observed between the emission spectrum of the donor (**4SPy**) and the  $S_0 \rightarrow S_2$  absorption band of the Bodipy **2** ( $J_{P_2}^{S_2} = 7.1 \times 10^{-3}$  cm). A noticeably weaker spectral overlap is seen with the  $S_0 \rightarrow S_2$  of **1** ( $J_{P_1}^{S_2} = 2.5 \times 10^{-3}$  cm) while, comparatively, the spectral overlap becomes nearly negligible with the  $S_0 \rightarrow S_1$  absorption bands of the Bodipys **1** and **2** ( $J_{P_1}^{S_1} = 4.7 \times 10^{-4}$  and  $J_{P_2}^{S_1} = 2.5 \times 10^{-4}$  cm).

## Femtosecond Upconversion

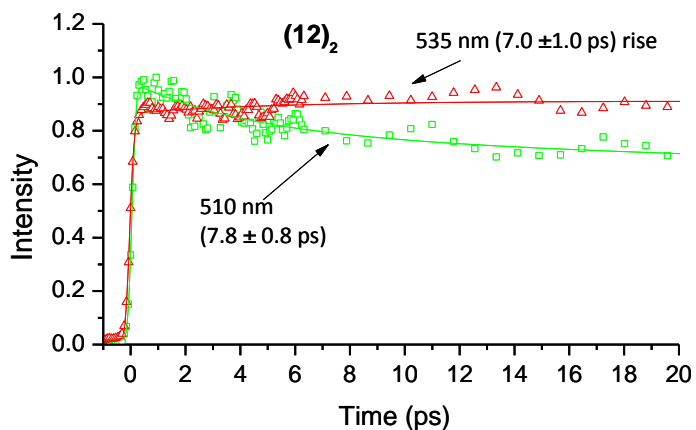


**Figure S15.** Fluorescence decays of  $(12)_2$  monitored at 510 nm and 535 nm respectively: Fits are shown with solid lines; excitation at 380 nm.

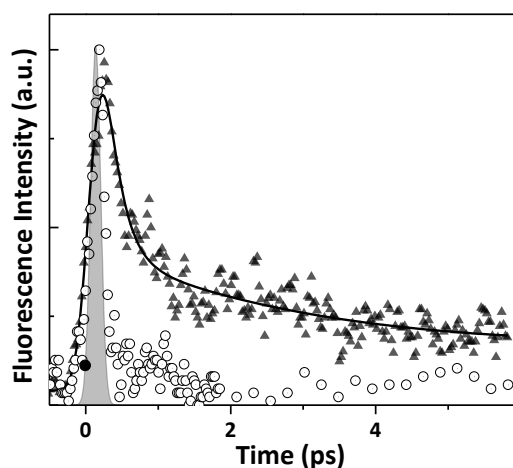
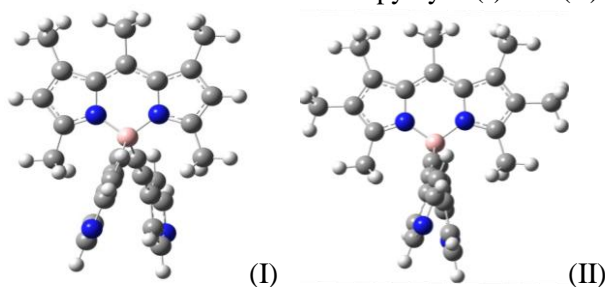


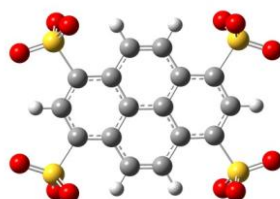
**Figure S16.** Dynamics of the fluorescence monitored at 420 nm; excitation at 380 nm (0-0 vibronic band of  $4SPy$ ). No fluorescence signal decaying within our temporal resolution ( $<140$  fs) was detected at 420 nm from the unoccupied cavitaand  $(12)_2$  ( $\circ$ ). The fluorescence decay of the complex  $4SPy-(12)_2$  at 420 nm  $\blacktriangle$  (originated from traces of unquenched  $4SPy$ ) is dominated by an ultrafast component of 0.18 ps (76%) along with two minor ones of 2.5 ps (16%) and 100 ps (8%) respectively.

## Theoretical Calculations

DFT calculations<sup>10</sup> have been carried out on the Bodipy dyes (I) and (II) and



the tetrasulfonated derivative of pyrene (**4SPy**)



Optimized geometries for the ground electronic states and absorption spectra have been calculated at the optimum geometry by TDDFT<sup>11</sup> calculations. All calculations have been carried out with the aid of Gaussian<sup>12</sup> 09 employing the B3LYP<sup>13</sup> functional and the 6-31G(d,p) basis set.

The calculated absorption spectra show that there is a near-degeneracy of the absorption peak of **4SPy** with the higher-energy absorption peak ( $S_2$ ) of **2**, see Fig. S17, indicating that the second excited state of the Bodipy **2** is relevant to the energy-transfer process. The calculated transition moments for  $S_0$ - $S_1$  (for I,II and **4SPy**) and  $S_0$ - $S_2$  (for I and II) are given in Table S2.

**Table S2:** Transition Dipole moments for  $S_0$ - $S_1$  (for I,II and **4SPy**) and  $S_0$ - $S_2$  (for I and II) in Debye

	x	y	z	Transition energy (nm) (f-value)
(I) $S_0$ - $S_1$ (in chloroform)	-0.0258 -0.0156	0.0353 0.0389	-2.0431 -2.6809	412.33 (0.3076) 422.03 (0.5174)
(I) $S_0$ - $S_2$ (in chloroform)	-0.0287 -0.0410	0.0954 0.1235	1.3896 0.9497	381.65 (0.1545) 367.66 (0.0759)
(II) $S_0$ - $S_1$ (in chloroform)	-0.0121 0.0031	0.0272 0.0301	-2.2207 -2.7503	430.26 (0.3482) 440.49 (0.5217)
(II) $S_0$ - $S_2$ (in chloroform)	-0.0223 -0.0262	0.1628 0.2280	1.4460 1.2417	381.17 (0.1688) 373.58 (0.1296)
( <b>4SPy</b> ) $S_0$ - $S_1$ (in chloroform)	0.0000 0.0000	0.0000 0.0000	-2.3945 -2.7851	376.74 (0.4623) 384.38 (0.6130)

**The z axis coincides with the long axis of the Bodipys and **4SPy**.**

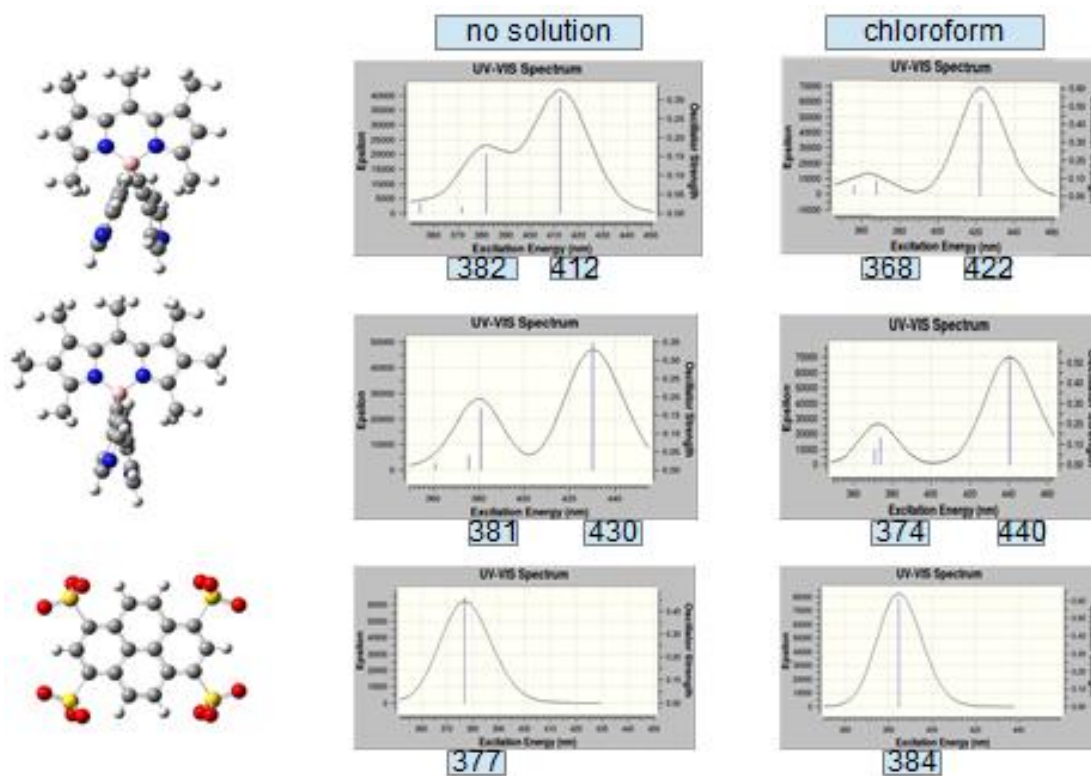


Figure S17. Calculated absorption spectra of Bodipys I, II and 4SPy.

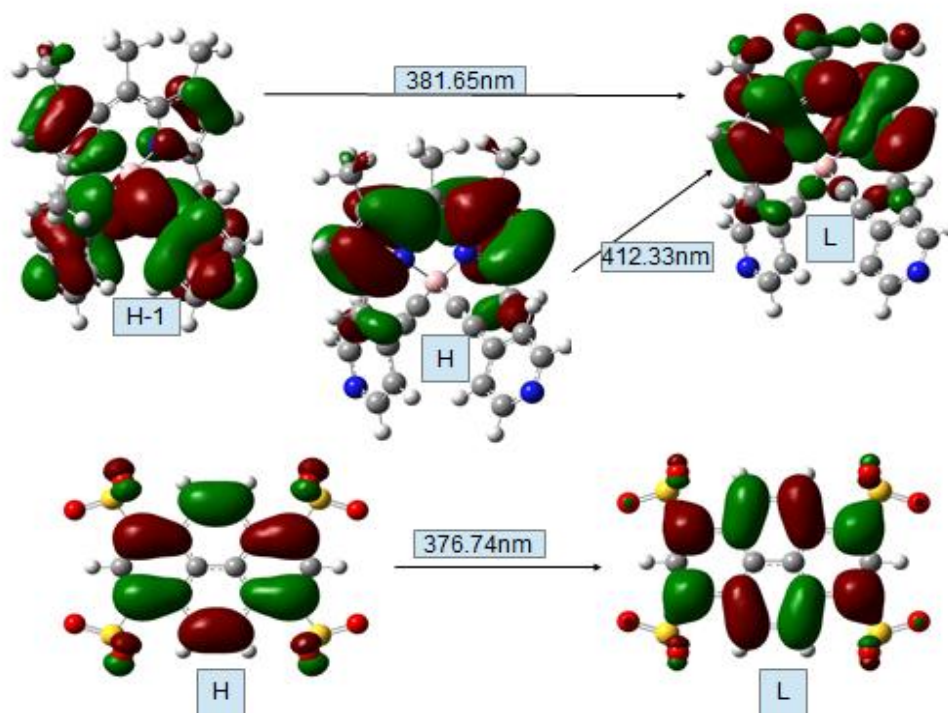
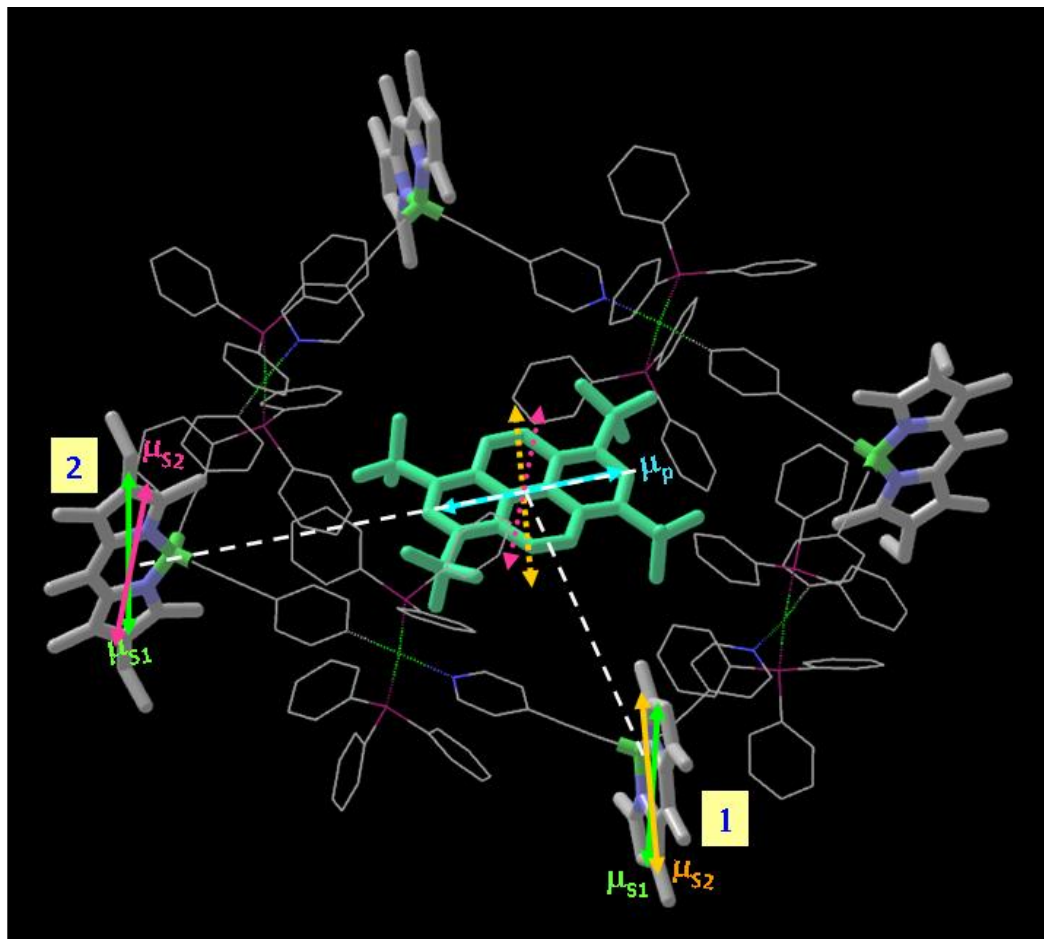


Figure S18. Molecular orbital picture of the relevant absorption transitions

### Chromophoric arrangement and dipole moments orientation

To assess and model the molecular geometry in the uninhibited liquid phase we have employed an optimized host-guest geometry free of strains compared to the highly warped molecular crystal structure. (MOPAC 2012 using the PM6 semiempirical method with the MOZYME function)<sup>7</sup>



**Figure S19.** Chromophoric arrangement and dipole moments orientation in the host-guest supramolecular assembly **4SPy-(12)<sub>2</sub>**.

The orientation factor is given by

$$\kappa = \cos(\theta_{DA}) - 3 \cos(\theta_D) \cos(\theta_A)$$

where  $\theta_{DA}$  is the angle between the donor and acceptor transition dipole moments  $\mu_D$  and  $\mu_A$  while  $\theta_D$  and  $\theta_A$  are their angles with respect to the vector connecting the D and A centers

The transition dipole moment of the  $S_1$  state of the Bodipys and 4SPy becomes completely polarized along the long molecular axis for each chromophore (see Table S2). Furthermore our findings, in consistency with experimental observations,<sup>14</sup> verify that the dipole moment vector of the  $S_0$ - $S_2$  optical transition of Bodipys inclines by  $\sim 10^\circ$  in plane with respect to the long molecular axis. On the basis of the above:

- the orientational factor  $\kappa$  becomes non – vanishing only for the dyad **4SPy – 2** in which the orthogonality between the transition dipole moments ( $\mu_p$  and  $\mu_2^{S_2}$ ) breaks down noticeably ( $\kappa=0.33$ ;  $\theta_D \approx 0^\circ$ ;  $\theta_{DA} \approx 80^\circ$ ;  $\theta_A \approx 80^\circ$ ).
- for the dyad **4SPy – 1**  $\theta_D \approx 90$  and  $\theta_{DA} \approx 90^\circ$ , so  $\kappa$  vanishes to  $\approx 0$ .

## X-ray Crystal Structure Determination

Crystals were grown by diffusion of EtOAc into a 1:1 CHCl<sub>3</sub>/DMF solution of the reactants forming the host and guest. X-ray diffraction data were collected by the rotation method at 100 K using synchrotron radiation at the XO6DA beam line (Swiss Light Source, Paul Scherrer Institut, Villigen, Switzerland) on a poor quality crystal of dimensions 0.3X0.2X0.1 mm.

Crystal structure determination of the complex

Crystal data. (C<sub>268</sub>H<sub>248</sub>B<sub>4</sub>N<sub>12</sub>P<sub>8</sub>Pt<sub>4</sub>) x 0.5 • (C<sub>16</sub>H<sub>6</sub>O<sub>12</sub>S<sub>4</sub>) x 0.5 • (C<sub>15</sub>H<sub>15</sub>N<sub>5</sub>O<sub>5</sub>) x 0.5, M = 22319.90, orthorhombic, a = 26.739(3), b = 47.581(3), c = 26.660(3) Å, V = 33919 (6) Å<sup>3</sup>, T = 100 K, space group Pccn (no.56), Z = 8, 151523 reflections measured, 13392 unique (R<sub>int</sub> = 0.044) which were used in all calculations. The final R<sub>1</sub> = 0.1285 for 11750 reflections with Fo > 4sig(Fo) and 0.1335 for all data (13392 reflections) and S = 1.955.

*Structure solution & Refinement:* Diffraction data up to 1.04 Å resolution were collected, processed by MOSFLM<sup>15</sup> and scaled with the SCALA<sup>16</sup> software, solved by direct methods and refined by the program SHELXL97<sup>17</sup>. By alternating cycles of restrained full-matrix least-squares refinement and manual inspection, the missing atoms of the host, as well as these of the guest and solvent molecules (2 molecules of DMF at full occupancy and one molecule at half occupancy) were found. The crystal was characterized by disorder due to the presence of solvent molecules (more than the ones used in the refinement) and of the numerous phenyl groups on the phosphorous atoms, thus the refinement of the structure was finished with restraints on the bond distances of these phenyls, but also of the Bodipys (restraints of bond distances of the aromatic rings within 1.40 Å). The phenyl groups were forced also to remain planar (FLAT in SHELXL97). All solvent distances were constrained also during the refinement. The above distance constrains were necessary for a smooth converged refinement, otherwise it resulted in oscillating shifts of the positional parameters. The non-H atoms were refined by anisotropic refinement. H-atoms were placed at idealized positions on the non-H atoms and refined by the riding model (UH = 1.20 or 1.25 UC).

## References:

- (1) A. Kaloudi-Chantzea, N. Karakostas, C. P. Raptopoulou, V. Psycharis, E. Saridakis, J. Griebel, R. Hermann and G. Pistolis, *J. Am. Chem. Soc.* **2010**, *132*, 16327–16329
- (2) M. Fischer., J. Georges, *Chem. Phys. Lett.* **1996**, *260*, 115-118
- (3) W. A. Melhuish., *J. Phys. Chem.* **1961** *65*, 229-235
- (4) M. Fakis., E. Stathatos, G. Tsigaridas, V. Giannetas, P. Persephonis, *J. Phys. Chem. C* **2011**, *115*, 13429-13437
- (5) M. Fakis, P. Hrobárik, E. Stathatos, V. Giannetas, P. Persephonis, *Dyes and Pigments* **2013**, *96*, 304-312
- (6) M. Shah, K. Thangaraj, M. L. Soong, L. T. Wolford, J. H. Boye, I. R. Politzer, T. G., Pavlopoulos *Heteroatom Chem.* **1990**, *1*, 389
- (7) MOPAC 2012, James J. P. Stewart, Stewart Computational Chemistry, Colorado Springs, CO, USA, [HTTP://OpenMOPAC.net](http://OpenMOPAC.net) (2012).
- (8) R.G. Alden, E. Johnson, V. Nagarajan, W.W. Parson, C.J. Law, R.G. Cogdell., *J. Phys. Chem. B* **1997**, *101*, 4667-4680
- (9) J.R. Lakowicz, *Principles of Fluorescence Spectroscopy*, Kluwer, Dordrecht, 1999
- (10) R. G. Parr, W. Yang, *Annu. Rev. Phys. Chem.* **1995**, *46*, 701.
- (11) M. A. L. Marques, E. K. U. Gross, *Annu. Rev. Phys. Chem.* **2004**, *55*, 427.
- (12) Gaussian 09, Revision A.1, Frisch, M. J. et al. Gaussian, Inc., Wallingford CT, 2009
- (13) A. D. Becke, *J. Chem. Phys.* **1993**, *98*, 5648; C. Lee, W. Yang, R. G. Parr *Phys. Rev. B.* **1989**, *37*, 785.
- (14) J. Karolin, L. B. A. Johansson, L. Strandberg, T. Ny, *J. Am. Chem. Soc.* 1994, *116*, 7801
- (15) A. G. W. Leslie, H. R. Powell *Evolving Methods for Macromolecular Crystallography*, *245*, 41-51, Springer **2007**
- (16) P. R. Evans, Scaling and assessment of data quality, *Acta Cryst.* **2005**, *D62*, 72-82,
- (17) G.M. Sheldrick,; SHELXL-97, Release 97–2, University of Göttingen, Germany **1997**.